3 Biotech (2025) 15:134
https://doi.org/10.1007/s13205-025-04295-5

ORIGINAL ARTICLE

Design, synthesis, and pharmacological evaluation of heteroaryl thiol-linked kojic acid derivatives as a novel class of acetylcholinesterase inhibitors for Alzheimer's disease therapy

Madan Singh[1] · Chandrabose Karthikeyan[1] · Digambar Kumar Waiker[2] · Akhilesh Tiwari[1] · Sushant K. Shrivastava[2] · Sérgio F. Sousa[3] · Duangnapa Kiriwan[3] · Fábio G. Martins[4] · Narayana Subbiah Hari Narayana Moorthy[1]

Received: 10 February 2025 / Accepted: 27 March 2025 / Published online: 18 April 2025

Abstract

Natural products have long served as versatile templates for discovering lead molecules against various targets of pharmacological interest. Kojic acid, a fungal metabolite epitomizes this versatility as it elicits broad-spectrum biological properties. Described herein is a series of heteroaryl thiol-linked kojic acid derivatives that demonstrate potent acetylcholinesterase (AChE) inhibition along with anti-amyloid-β (Aβ) aggregation activity and blood brain barrier (BBB) permeability highlighting their potential as a novel class of Anti-Alzheimer's therapeutics. Seventeen kojic acid derivatives, synthesized by incorporating three different heterocyclic thiols, were evaluated for in vitro AChE inhibition employing Ellman's method. The most potent analogs identified from the AChE inhibition studies were further evaluated for binding to the peripheral anionic site (PAS) of AChE using the propidium iodide (PI) displacement assay, anti-amyloid-β (Aβ) aggregation inhibition using the thioflavin T assay, and BBB permeability using the PAMPA-BBB assay. Obtained findings indicated that two compounds **MS 21–05** and **MS 21–11** bearing a 5-methoxybenzo[d]thiazol-2-yl)thio moiety and 5-phenyl-1,3,4-oxadiazol- 2-yl) thio moiety, respectively, elicited potent AChE inhibition (IC_{50} < 5 µM), moderate anti-Aβ aggregation effects and good BBB permeability. The molecular docking studies of compound **MS 21 - 11** along with its molecular dynamics simulations at peripheral anionic site (PAS) of enzyme AChE provided structural insights into the binding mode of these derivatives. Taken together, the findings of this study establish heteroaryl thiol-linked kojic acid derivatives as a valuable molecular framework for developing anti-Alzheimer's therapeutics that target both cholinergic dysfunction and amyloid-β aggregation.

Keywords Alzheimer's disease · Kojic acid derivatives · Acetylcholinesterase inhibitors · Molecular dynamic simulations · Aβ-aggregation inhibition

Introduction

Alzheimer's disease (AD) is a neurodegenerative disorder that is accompanied by decline in both communication and cognitive abilities as well as behavioural changes in affected individuals (Tripathi et al. 2024); (DeTure and Dickson 2019). Currently, 57 million cases of AD are reported worldwide, and this number is expected to rise to 153 million by the year 2050 (Nichols et al. 2022). The majority of these cases occur in persons aged 60 or above causing physical, financial, and emotional trauma to both the patient and the caregivers (Vu et al. 2022). The etiology of AD remains unknown which makes drug discovery for this disease very challenging (Abdallah 2024). Several hypotheses have been formulated to understand AD pathogenesis including cholinergic dysfunction, amyloid-β (Aβ) plaques formation,

✉ Narayana Subbiah Hari Narayana Moorthy
hari.nmoorthy@gmail.com

1 Cancept Therapeutics Laboratory, Department of Pharmacy, Indira Gandhi National Tribal University, Amarkantak 484887, India

2 Pharmaceutical Chemistry Research Laboratory, Department of Pharmaceutical Engineering and Technology, Indian Institute of Technology (Banaras Hindu University), Varanasi, UP 221005, India

3 UCIBIO—Applied Molecular Biosciences Unit, BioSIM-Departamento de Biomedicina, Faculdade de Medicina, Universidade do Porto, 4200319 Porto, Portugal

4 Associate Laboratory i4HB—Institute for Health and Bioeconomy, Faculdade de Medicina, Universidade do Porto, 4200319 Porto, Portugal

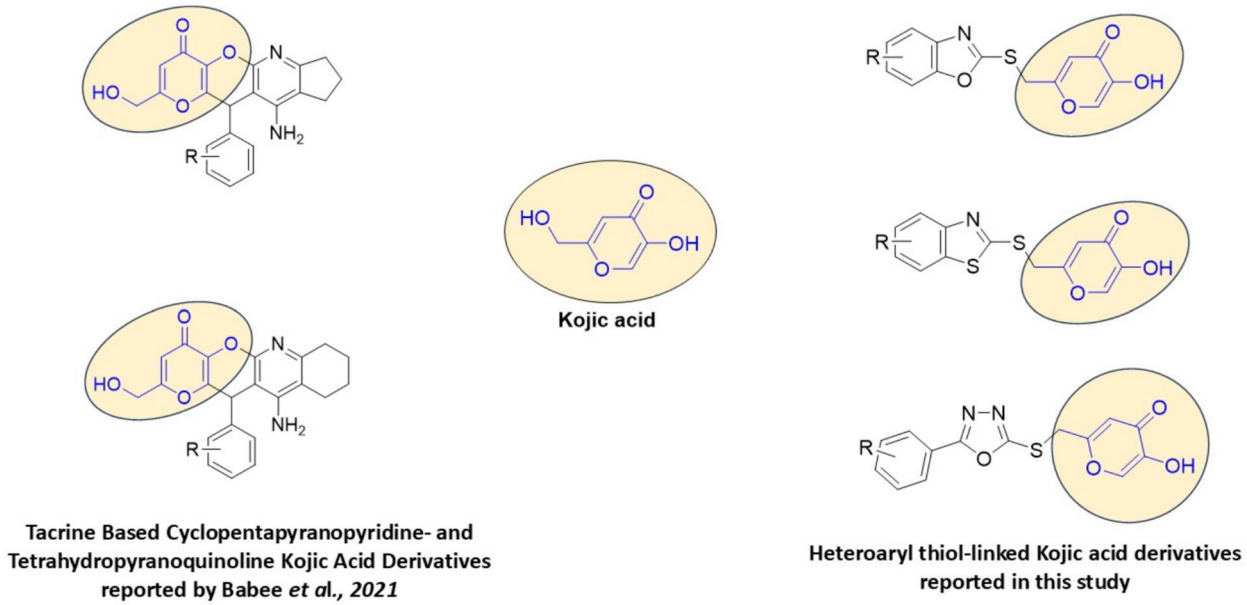

Fig. 1 Kojic acid derivatives as acetylcholinesterase inhibitors

activation of N-methyl-D-aspartate receptor (NMDAR) mediated neuroinflammation and monoamine oxidase (MAO) activation, all of which emphasizes the multifactorial nature of the disease (Fan et al. 2020; Rai et al. 2020).

Cholinergic dysfunction involving declined cholinergic transmission and Aβ-aggregation, is one of the most explored areas in AD pathogenesis (Zuin et al. 2022). Acetylcholinesterase (AChE), a serine hydrolase enzyme responsible for acetylcholine (ACh) hydrolysis, has been closely associated with cognitive decline due to the reduction of ACh levels (García-Ayllón et al. 2011). AChE is a key contributor for enhanced deposition of Aβ-aggregates observed in Alzheimer's disease (García-Ayllón et al. 2011; Ramakrishna et al. 2024). The accumulation of Aβ fibrils and oligomers in brain disrupts cell communication, potentiate neuroinflammation while causing progressive neuritic damage, ultimately leading to cognitive dysfunction and neuronal impairment (DeTure and Dickson 2019). Furthermore, Aβ accumulation in neuronal cells causes oxidative stress in mitochondria through the generation of free radicals which ultimately exacerbates brain damage (Foret et al. 2024). Over the past several years, numerous AChE inhibitors have been discovered, paving the way for an enhanced therapeutic strategy to ameliorate cognition linked with AD. Numerous naturally derived AChE inhibitors have been isolated from diverse sources, such as plants, fungi, and marine alkaloids, with the majority being alkaloids that have heterocyclic scaffolds, including indole, isoquinoline, quinolizidine, and piperidine (Ana Paula et al. 2013). Nevertheless, efforts to identify novel scaffolds with AChE inhibitory potency are still ongoing (Obaid et al. 2022).

Kojic acid (chemically 5-hydroxy- 2-(hydroxymethyl)– 4*H*-pyran- 4-one) is a natural metabolite isolated from fungi that has been recently recognized as a medicinally important scaffold endowed with broad-spectrum pharmacological properties (Saeedi et al. 2019; Brtko 2022). Kojic acid derivatives have been shown to possess a variety of biological properties, including antioxidant, anti-inflammatory, anti-tyrosinase, anticancer, and antibacterial activities, among others. (Saeedi et al. 2019; Brtko 2022; Emami et al. 2022). Most importantly, novel tacrine-based kojic acid derivatives have shown promised as anti-AChE agents with potential therapeutic applications in AD (Babaee et al. 2021) (Fig. 1). The authors fused kojic acid with a 6,7,8,9-tetrahydro-4*H*-pyrano[2,3-b]quinolin- 5-amine moiety to develop tacrine-based cyclopentapyranopyridine and tetrahydropyranoquinoline-kojic acid derivatives with acetylcholinesterase inhibitory potency (Babaee et al. 2021) (Fig. 1). The primary goal of this research project aimed to design some new potent molecules that effectively inhibit AChE based on kojic acid using a medicinal chemistry approach that preserves the biologically important γ-hydroxy pyrone ring while linking several heterocyclic rings via the flexible 2-hydroxymethyl group. To this end, we effectively designed, synthesized, and screened a series of novel kojic acid analogs conjugated with diverse heterocyclic thiols for their anti-Alzheimer's properties, focusing on AChE inhibition, having the capacity to suppress AChE-induced Aβ aggregation and having the capability to cross the blood–brain barrier (BBB). Additionally, the binding mechanism of these analogs to AChE was analyzed using molecular docking experiments in conjunction with molecular dynamics

simulations. The findings from these comprehensive investigations are discussed herein.

Experimental

Chemistry

All the chemicals as well as solvents required for the synthesis of the target compounds were procured commercially and were used without any purification. NMR spectra (^{1}H and ^{13}C NMR) of the synthesized compounds were recorded on a JNM-ECZ500R/S1 FT NMR (Jeol, Japan) and the chemical shift (δ) is reported in part per million (ppm). HR-MS analysis of the synthesized compounds was performed using mass spectrometer X 500R QTOF HRMS (Sciex, Singapore). The IR spectrum of the synthesized molecules was obtained using a spectrometer of Alpha-II Eco ATR (Bruker, Germany). Melting points are reported uncorrected and measured using an EI digital melting point instrument. Thin-layer chromatography (TLC) with silica-coated aluminum plates (Kieselgel 60 F254, Merck, Germany) was employed for monitoring reaction progress and the reaction zones were visualized under ultraviolet (UV) light.

Synthesis of chlorokojic acid (2) (He et al. 2021)

Initially, kojic acid (**1**, 35 mmol, 4.97 g) was slowly mixed into, 20 mL of thionyl chloride with continuous stirring at ambient temperature for 2 h. After which, the chemical mixture was subsequently allowed to cool down at room temperature and the solid precipitate that formed was filtered out and washed with petroleum ether. The precipitate obtained was dried under a vacuum to give chlorokojic acid as a white solid.

General protocol for the synthesis of 2-(heteroaryl thio)methyl)−5-hydroxy-4*H*-pyran-4-ones (MS 21–01 to MS 21–17) (Rakse et al. 2013)

To a reaction flask containing an equimolar mixture of chlorokojic acid **(2)** (0.160 g, 1 mmol) and a heterocyclic thiol (1 mmol) in 20 mL of acetone and K_2CO_3 (0.207 g, 1.5 mmol) was mixed and refluxed for 6–9 h. The excess solvent was evaporated to form a concentrated mixture after completion of the reaction. It was then diluted with 200 mL of distilled water and acidified with 10% hydrochloric acid until a precipitate was formed. Subsequently, it was filtered out and, thoroughly rinsed using cold distilled water and dried. The obtained product was then recrystallized using an equal amount of ethyl acetate and hexane to get the title compounds as pure products. (Please refer to supplementary data for characterization data and the spectra of synthesized compounds).

Table 1 AChE inhibitory activity of heteroaryl thiol-linked kojic acid derivatives (MS 21–01 to MS 21–17)

S. No	Compound code	X	R	hAChE IC_{50} ± SEM (μM)[#]
1	MS 21–01	S	H	2.419 ± 0.026
2	MS 21–02	S	6-NO_2	2.863 ± 0.038
3	MS 21–03	S	5-Cl	1.568 ± 0.032
4	MS 21–04	S	6-OC_2H_5	1.372 ± 0.021
5	MS 21–05	S	5-OCH_3	1.225 ± 0.019
6	MS 21–06	O	H	1.309 ± 0.041
7	MS 21–07	O	6-Cl	1.495 ± 0.027
8	MS 21–08	O	5-Cl	3.213 ± 0.024
9	MS 21–09	O	5-CH_3	1.279 ± 0.032
10	MS 21–10	O	5-NO2	1.467 ± 0.027
11	MS 21–11	–	H	1.035 ± 0.029
12	MS 21–12	–	4-F	1.622 ± 0.021
13	MS 21–13	–	4-OH	4.934 ± 0.018
14	MS 21–14	–	4-OCH_3	3.926 ± 0.038
15	MS 21–15	–	4-CH_3	4.296 ± 0.022
16	MS 21–16	–	4-NO_2	2.816 ± 0.018
17	MS 21–17	–	4-Br	1.774 ± 0.036
18	Donepezil			0.044 ± 0.007

[#]All experiments were performed in triplicate (n = 3)

Biology

In vitro cholinesterase inhibition assay

To evaluate the AChE inhibition potential of the synthesized compounds, in vitro AChE inhibition assay was performed using Ellman's method with slight modification in the protocol (Ellman et al. 1961; Singh et al. 2021; Waiker et al. 2024). The hAChE (source human erythrocyte, EC.No 3.1.1.7), acetylthiocholine iodide (ATCI, CAS No. 1866 - 15- 5) and 5,5′-dithiobis- 2-nitrobenzoic acid known as Ellman's reagent (DTNB CAS No.69–78-3) were purchased from Sigma Aldrich, U.S.A.. Five different concentrations of compounds (10 µL each) were treated with 50 µL of enzyme (0.022 U/mL) and a solution of ATCI (30 µL; 1.5 mM) at room temperature. Ellman's reagent (160 µL; 0.15 mM) was added to this mixture at the end of the assay and the absorbance was measured at a wavelength of 412 nm. Non-enzymatic hydrolysis of the substrate was measured using a blank sample with the same procedure without the enzyme. Donepezil was employed as a reference compound in the assay. Each experiment was performed in triplicates and the findings are presented in Table 1.

Propidium iodide (PI) displacement assay

The PI displacement assay was employed to determine the competitive binding efficacy of the compounds **MS 21–05** and **MS 21–11** to PAS-binding region of AChE in comparison to propidium iodide (TAYLOR et al. 1974; Peauger et al. 2017). In this assay, AChE (5U) is incubated with (at 10 µM and 50 µM concentrations (150 µL)) and without inhibitors for period of 6 h at 25 °C. Add 50 µL of PI (1 µM) to this reaction mixture, adjust the final volume up to 200 µL and then incubated the reaction mixture for 10 min. The fluorescence intensity was quantified utilizing a BioTek Synergy (USA) fluorescent plate reader at excitation and emission wavelengths of 535 nm and 595 nm, respectively.

Anti-Aβ aggregation activity by thioflavin T assay

Compounds **MS 21–05** and **MS 21–11** were further evaluated for their Aβ-aggregation inhibitory properties via AChE-induced and self-induced protocols (Verma et al. 2024). Aβ (1–42 peptide) procured from (Cayman, U.S.A.) was mixed with dimethylsulfoxide (DMSO) to get a stock solution of 1 mM that was subsequently diluted with 7.4 pH phosphate buffer saline (PBS) to attain an actual working concentration of approximately 10 µM. The compounds **MS 21–05** and **MS 21–11** were mixed into DMSO to obtain the stock solutions, which was further diluted with PBS to maintain a final DMSO content less than or equal to 1% (w/v).The Aβ-aggregation inhibitory activity (Aβ, 10 µM) on various concentrations of 5, 10 and 20 µM in triplicate experiments were evaluated using Aβ-to-inhibitor molar ratios at 10:5, 10:10, and 10:20 µM, respectively.

Self-induced amyloid-beta aggregation assay Furthermore, Aβ aggregates were generated for self-induced amyloid-beta aggregation inhibitory study by incubating a 50 µM Aβ solution made in 7.4 pH PBS at 37 °C for a duration of 48 h in both conditions either including or excluding the inhibitors (5, 10 and 20 µM), followed by addition of Thioflavin T solution (100 µM) prepared using 8.0 pH of glycine–NaOH buffer. The appropriate wavelengths such as 450 nm and 485 nm were utilised to determine fluorescence intensity. Using the following formula the % inhibitory activity was determined.

$$\% \text{ Inhibition} = \left[100 - \left(F_i/F_o \times 100\right)\right]$$

where Fi and Fo stand for the presence and absence of the inhibitor, respectively.

Human AChE-induced amyloid-beta (Aβ) aggregation assay With exception of adding human AChE at a 1:100 molar ratio to Aβ (10 µM) using 7.4 pH phosphate buffer saline (pH 7.4), the same procedure as the self-induced anti-Aβ aggregation experiment was used for hAChE-induced amyloid-beta aggregation assay.

In vitro PAMPA-BBB assay

The blood–brain barrier permeability of the most potent compounds **MS 21–05** and **MS 21–11** was evaluated using a PAMPA-BBB assay (Di et al. 2003; Tsinman et al. 2011; Shrivastava et al. 2022). In brief, a PVDF membrane (pore size: 0.45 µm) precoated with porcine brain-derived lipid (4 µL, 20 mg/mL) was prepared on acceptor microplate and filled with 200 µL of PBS (pH7.4): ethanol (7:3 v/v). The test compounds were dissolved in same PBS:ethanol mixture (200 µL) were loaded onto a donor microplate. After that, both acceptor and donor plates were placed collectively at 25 °C for 18 h, which permit passage of the investigated molecules from donor plate to acceptor plate using a PVDF membrane and finally absorbance of all three plates including, reference, acceptor and donor plates were measured using spectrophotometer and all measurements were performed in triplicate. The results obtained were further validated by comparison with the reference drugs having established BBB permeabilities.

In silico studies

Molecular docking

The three-dimensional structure of human acetylcholinesterase (hAChE) co-crystallized with inhibitor donepezil (PDB code: 6O4 W; resolution: 2.35 Å) was obtained from the Protein Data Bank (Gerlits et al. 2019). The designed inhibitors were sourced from the experimental laboratory and subsequently prepared using Open Babel (O'Boyle et al. 2011).

In this study, structure-based ligand docking calculations were performed using GOLD software version 2022.0.1 (Verdonk et al. 2003), employing four scoring functions: ASP, ChemPLP, Goldscore, and Chemscore. The docking parameters were optimized during various redocking experiments and included the center and dimensions of the docking box, as well as the number of independent GA runs.

Re-docking is a reproducible and reliable method used to evaluate and refine the docking protocol. In this technique, a reference ligand is removed from the protein–ligand crystal structure complex, and a protein–ligand docking protocol is employed to estimate the ligand's correct pose within the binding pocket. The similarity between the re-docked and crystallographic poses was evaluated using Dock RMSD through comparison of root mean square deviation (RMSD) values of the heavy atoms of the ligand in both poses (Bell

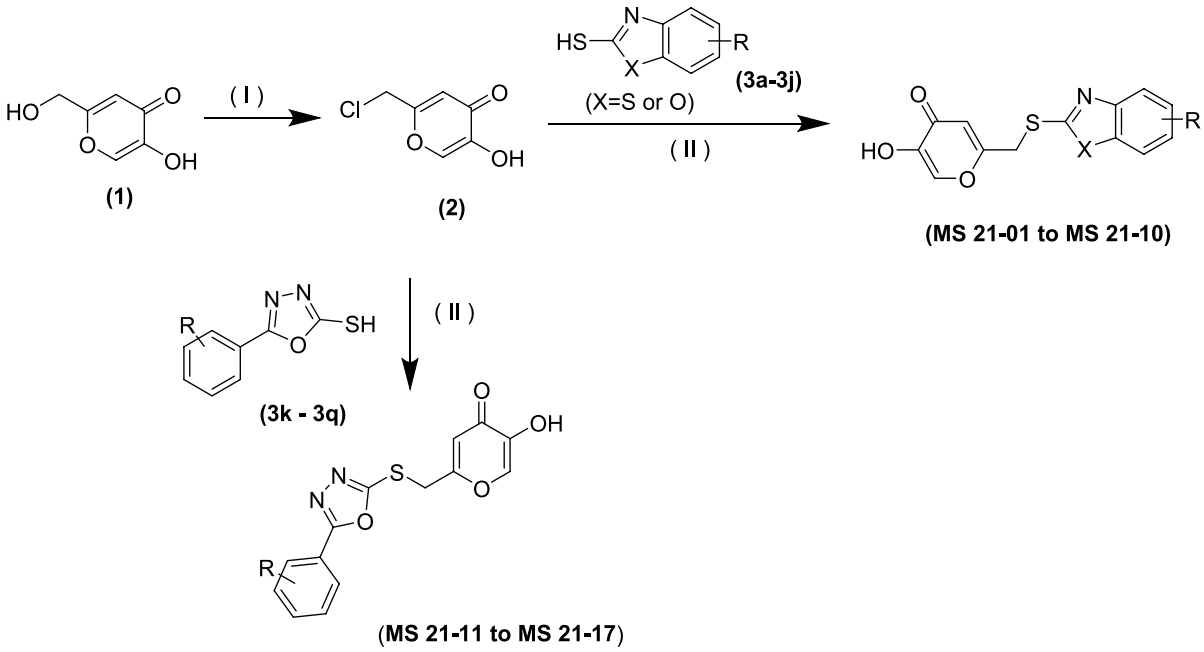

Scheme 1 Synthesis pathway for 5-hydroxy- 2-(heteroaryl)thio)methyl)−4*H*-pyran- 4-ones (MS 21–01 to MS 21–17)

and Zhang 2019). The protocols which achieved an RMSD ≤2 Å for each scoring function were selected for subsequent steps.

The docking protocol, once optimized, was then applied using the same parameters in the virtual screening. The top hits were selected for further evaluation at the atomic level using molecular dynamics simulations.

MD simulations

In order to investigate the molecular behaviour, related to protein and ligand interactions over time, molecular dynamics (MD) simulations were conducted. MD simulations, performed using the Amber20 software package (Case et al. 2005), to evaluate the interactions between the protein and the best performing docked ligands. LEAP was used to build the topology and parameters of the ligands with the general AMBER force field (Wang et al. 2004). A periodic boundary condition with a minimum distance of 12 Å was established for every system. The box was solvated using a TIP3P water mode. Long-range electrostatic interactions were calculated using the Ewald summation technique with particle mesh. A cut-off value 10.0 Å was chosen as for both the electrostatic and Lennard Jones interactions. The SHAKE approach was used to constrain all hydrogen atom bonds. This made it possible to use a 2-fs time step.

A four-step energy minimization procedure was applied to every protein–ligand complex. The minimisation approach alternated between the conjugate gradient and the steepest decline at the midpoint of each step and the first three steps, which each step involved up to 2500 cycles. Only water molecules were eliminated in first stage, while only hydrogen atoms during second stage. In order to maximise the amino acid side chains, the third step entailed restricting the protein backbone, followed by a final step where all constraints were removed for full system optimization.

During post-minimization, canonical ensemble (NVT) with a constant volume was used for a 50 ps equilibration phase. The Langevin thermostat was used to raise the system's temperature to 310.15 K slowly. Then, there was another equilibration of 50 ps in the NVT ensemble at 310.15 K. The production phase was then conducted for 200 ns at 310.15 K and 1 bar of pressure controlled by the Berendsen barostat utilising the isothermal-isobaric ensemble (NPT).

Free energy calculations

To estimate the binding free energies of the ligands against hAChE, the Molecular Mechanics Poisson-Boltzmann Surface Area (MM-PBSA) method was employed, utilizing the MM/PBSA python script available in AMBER (Miller et al. 2012). The final 100 ns of the Molecular dynamic simulations, comprising 500 frames per system, served as the basis for the computations. The exterior dielectric constant 80.0, the internal dielectric constant 4 and the ionic strength

0.100 mol dm^{-3} were used. Using per-residue decomposition analysis, local interactions between each ligand and protein were further assessed.

Results and discussion

Chemistry

The 5-hydroxy-2-(heteroaryl)thio)methyl)−4*H*-pyran-4-one**s (MS 21–01 to MS 21–17)** were synthesized via a multistep reaction as illustrated in Scheme 1. Reaction of the commercially available starting material kojic acid **(1)** with thionyl chloride at room temperature yielded the key intermediate chlorokojic acid **(2)** in excellent yield. The obtained chlorokojic acid (**2**) was then reacted with substituted benzo[d]thiazole- 2-thiol or benzo[d]oxazole-2-thiol, 5-(phenyl)−1,3,4-oxadiazole- 2-thiols in a basic environment in order to obtain desired molecules. The synthesized molecules were characterized through IR, NMR, and HR-MS spectroscopy, and the resulting data confirmed the successful synthesis of the desired heteroaryl-thiol-linked kojic acid derivatives.

Biological evaluation

The synthesized compounds were evaluated for their AChE inhibitory potential in vitro using Ellman's protocol (Waiker et al. 2023; Tripathi et al. 2019), with donepezil as the positive control. Table 1 displays the outcomes of this experiment. As evident from Table 1, all the synthesized kojic acid derivatives showed potent AChE inhibition (< 5 µM), with IC_{50} values between 1.035 µM and 4.93 µM. Among the three classes of heterocyclic thio ethers studied, kojic acid derivative containing 5-(phenyl)− 1,3,4-oxadiazole moieties displayed potent acetylcholinesterase inhibitory potency having IC_{50}value of 1.035 ± 0.029 µM. Substitution on the phenyl group drastically decreased the potency, and the least activity observed for the kojic acid derivative with a 4-hydroxyl substitution at phenyl ring linked with oxadiazole moiety. In contrast, for kojic acid derivatives containing the benzothiazole moiety, substitution on the benzo ring of the benzothiazole moiety with either chloro or alkoxy groups increased potency. While, in the case of kojic acid derivatives with benzoxazole moiety, where methyl substitution in the benzoxazole ring's C5 led to a slight enhancement in acetylcholinesterase inhibitory activity, a similar pattern was not seen. Preliminary SAR studies revealed that compounds **MS 21–05** and **MS 21–11** as promising lead molecules for further studies.

Next, we investigated the identified lead molecules **MS 21–05** and **MS 21–11** for their ability to bind to the peripheral anionic site (PAS) of acetylcholinesterase using a propidium iodide displacement assay (Ramrao et al. 2021). Propidium iodide (PI) is a well-recognized ligand that specifically binds to the PAS region of AChE, effecting an 8 to 10 fold increase in fluorescence intensity (Silva et al. 2013). Competitive inhibitors that bind to the PAS of AChE can cause a reduction in fluorescence intensity signifying the displacement of PI from the site. As the association of PAS with the nonamyloidogenic form of Aβ leads to Aβ accumulation and the formation of fibrils, molecules that bind to this region are anticipated to retard β-amyloid aggregation, which is therapeutically beneficial in the AD. The data presented in Table 2 show the % PI displacement by the lead molecules **MS 21–05** and **MS 21–11** at three distinct levels (10, 20, and 50 µM). Obtained results indicate that PI displacement from AChE site was enhanced with the increasing concentrations of both compounds which was comparable to donepezil at all tested concentrations. This finding suggested that the binding of both lead molecules with AChE-PAS site may contribute in anti-Aβ aggregation effects of molecular scaffolds.

Furthermore, several reports have highlighted the role of AChE in promoting Aβ aggregation through selective interaction with PAS (Verma et al. 2024). Drug molecules that bind to PAS of AChE may impede the Aβ aggregation and deposition in the brain. Hence, we evaluated the anti-Aβ aggregation potential of lead molecules **MS 21–05** and **MS 21–11**, we did a Thioflavin T-based fluorometric test. In this experiment, three different Aβ:inhibitor molar ratios (10:5, 10:10, and 10:20 µM) were employed. As compared to donepezil in self- and AChE-induced experiments, both lead molecules demonstrated a moderate increase in percentage anti-Aβ aggregation effects and a reduction in NFI at all three tested concentrations (5, 10, and 20 µM), according to the results, which are shown in Fig. 2 as percentages of aggregation of amyloid-beta inhibition and normalised fluorescence intensity (NFI). These findings further suggested

Table 2 The PI displacement assay and PAMPA-BBB permeability data of lead molecules MS 21–05 and MS 21–11

Compound code	PI displacement from PAS-hAChE (%)			PAMPA-BBB permeability	
	10 µM	20 µM	50 µM	$Pe_{(exp)}$ (10^{-6} cm s^{-1})	Prediction
MS 21–05	17.211 ± 1.008	20.427 ± 1.009	29.408 ± 1.512	5.756 ± 0.035	CNS^{+a}
MS 21–11	19.141 ± 1.074	23.107 ± 1.071	32.137 ± 1.142	5.941 ± 0.032	CNS^{+a}
Donepezil	24.762 ± 1.101	33.014 ± 1.031	46.043 ± 1.081	6.832 ± 0.041	CNS^{+a}

[a]CNS^{+} indicates good BBB permeability

that both the lead molecules possess anti-Aβ aggregation potential as well.

Finally, we evaluated blood–brain barrier (BBB) permeability of the lead molecules as it is a critical factor in anti-Alzheimer's drug discovery. Any molecule that demonstrates potent AChE inhibition must be able to cross the BBB to be effective. Therefore, we investigated the BBB permeability of the two identified lead molecules using the in vitro PAMPA-BBB assay method (Di et al. 2003; Srivastava et al. 2019). This assay evaluates the passive diffusion of a substance from donor to acceptor compartment, which is partitioned through brain (porcine brain) lipid membrane. The assay is initially validated using a set of marketed drugs to establish a permeability threshold across the membrane. Higher permeability coefficient (Pe) compounds (> 4.6 $\times 10^{-6}$ cm/s) were generally thought to exhibit excellent brain permeability, while uncertain compounds having (Pe values between 1.7 and 4.6 $\times 10^{-6}$ cm/s) and compound with poor permeability (Pe values less than 1.7 $\times 10^{-6}$ cm/s) were classified. Both compounds **MS 21–05** (Pe = 5.756 ± 0.035 $\times 10^{-6}$ cm/s) and **MS 21–11** (Pe 5.941 ± 0.032 $\times 10^{-6}$ cm/s) demonstrated excellent BBB permeability as presented in Table 2. These findings further support anti-Alzheimer's potential with good BBB permeability of the lead molecules.

In silico studies

Molecular docking and molecular dynamic simulations were employed to understand the binding mechanism of the 5-hydroxy- 2-(hydroxymethyl)− 4*H*-pyran- 4-one derivatives with AChE. To determine the most suitable docking approach for the structure of hAChE with donepezil complex, several parameters, including the scoring functions and number of genetic algorithms (GA) runs (ranging from 10 to 100). RMSD of re-docking runs are displayed in Table 3.

Table 3 shows that crystallographic pose was properly recreated by all scoring functions, all generated poses with RMSD values of smaller than 1 Å. However, in terms of computational time per docking simulation, Goldscore required four times longer than ChemPLP. Based on these observations, we selected the ChemPLP scoring function, configured with 100 GA runs, for the docking studies. This choice was guided by ChemPLP's demonstrated accuracy, shorter computational time, and more precise binding affinity scores compared to the other scoring functions, which collectively enhance computational efficiency.

All the screened compounds were compared with donepezil a known inhibitor for comparison (pIC_{50} of 8.8 and docking score of 106.9 kcal/mol), (Darsey and Masarweh 2020). The IC_{50} values were converted to pIC_{50} values, ranging from 5.3 to 6 (higher values indicate better performance). In the end, compound **MS 21–11** was selected based on their pIC_{50} values.

Compound **MS 21–11** in the MS 21 series, with the highest pIC_{50} of 5.9 and docking score of 79.6 kcal/mol. Because of the overlapping pIC_{50} values, discriminating between high and low performers proved difficult. Nonetheless, we chose compound **MS 21–11** for further analysis. Based on the obtained results, compound **MS 21–11** was selected for a detailed analysis of molecular interactions using molecular dynamics simulations, with donepezil as the reference ligand.

RMSD calculations were used during simulation to evaluate protein–ligand complex's stability. All systems stabilized after 100–200 ns of simulation, indicating that the protein–ligand complexes had reached equilibrium as shown in Fig. 3. In all the simulations for various compounds, the RMSDs for protein remained below 2.5 Angstrom, indicating that the protein–ligand complex systems were well equilibrated after 50 ns. For the known drug donepezil, the RMSD values initially increased significantly during the first 50 ns and then stabilized, fluctuating around 2–2.5 Angstrom for until the end simulation time. After 100 ns, the RMSD value for the Compound **MS 21–11** was obtained.

Furthermore, as shown in Table 4, Solvent Accessible Surface Area (SASA) calculation showed that all compounds were buried in the binding pocket between a degree of 71% and 92%. Compound **MS 21–11** exhibited the highest percentage of burial (92.8%) among the selected ligands, while donepezil had the lowest percentage (77.9%).

Since ligands bonded to protein and all protein–ligand complexes were stable, the MM-PBSA method was used to assess the binding energy. Results indicated that selected compound **MS 21–11** had better predicted ΔG binding values compared to the reference compound. The compound **MS 21–11** had predicted ΔG binding values of − 36.6 ± 0.1 kcal/mol, respectively.

To further elucidate the interactions between these compounds and the hAChE protein, a per-residue decomposition analysis was performed. This analysis identifies which amino acids are most influential in interaction of ligands with protein target. Based on the MM-PBSA results, we ranked the residues of the binding site according to their interactions with the ligands and their contributions for the whole bound energy. According to Table 4, which revealed that the components with the binding energy are explained in depth using hydrogen bonds and hydrophobic interactions. Trp83 was observed as the most common interacting residue. Residues Trp83, Gly118, Phe335 and Tyr338, which are important for the binding of the known ligand donepezil, are also involved in binding with the designed compounds. This suggests that the designed compounds engage with same key residues in pocket site known as ligand.

Two-dimensional interaction was used to elucidate binding interaction of these selected with residues of hAChE binding pocket predicted by MD analysis.

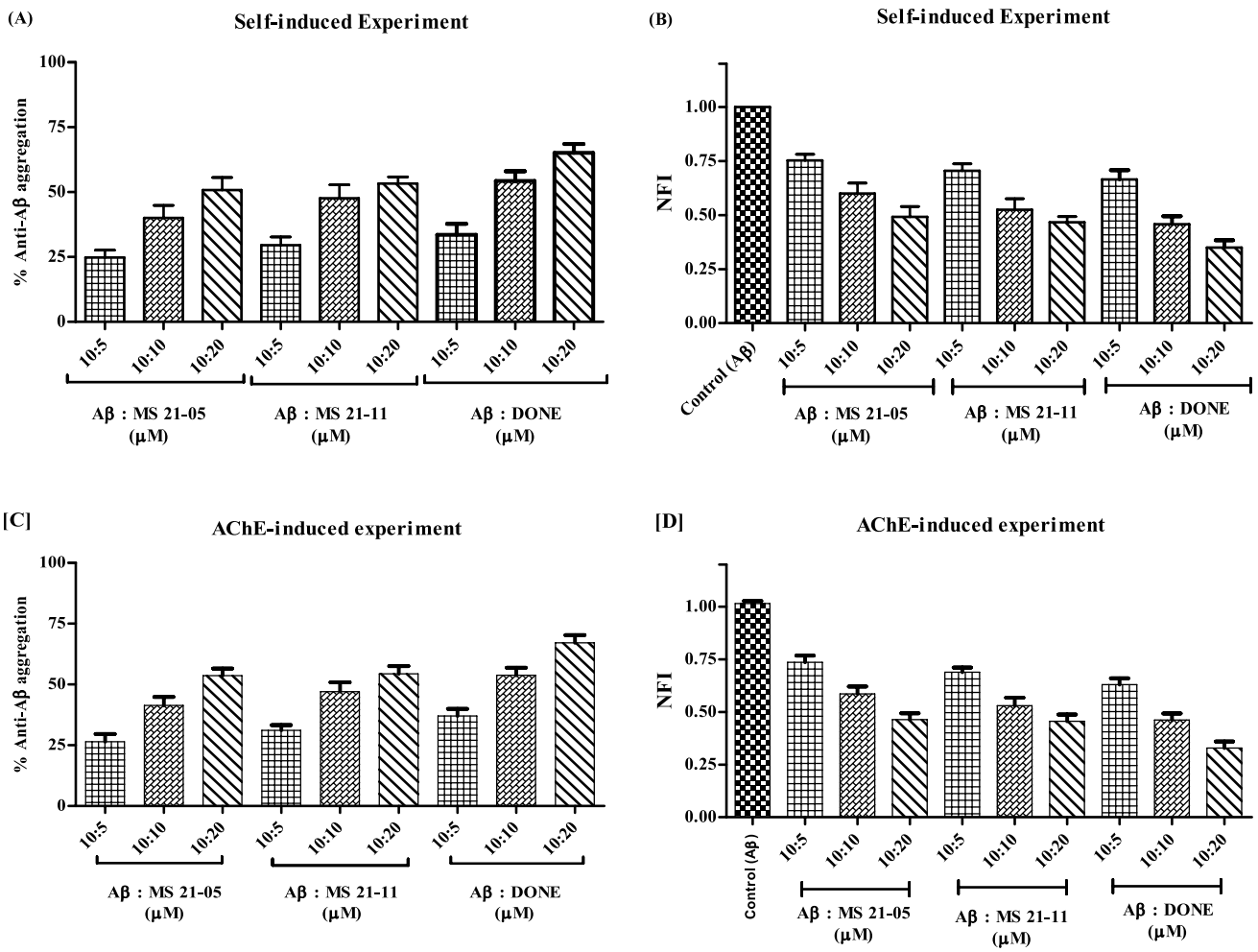

Fig. 2 Anti-Aβ aggregation effect of compound MS 21–05, MS 21–11 and donepezil: **A** self-induced % anti-Aβ aggregation experiment; **B** NFI in self-induced experiment; **C** hAChE-induced anti-Aβ aggregation experiment and **D** NFI in hAChE-induced anti-Aβ aggregation experiment. Results are represented as mean ± SEM of three independent experiments ($n = 3$)

Table 3 Calculation of various docking poses of donepezil with hAChE such as docking scores, RMSD values, and computation times were determined by varying the scoring functions and the number of GA runs performed to optimize the docking performance using GOLD software

GA run	ASP			Goldscore			ChemPLP			Chemscore		
	Score	RMSD (Å)	Time (s)	Score	RMSD (Å)	Time (s)	Score	RMSD (Å)	Time (s)	Score	RMSD (Å)	Time (s)
10	67.1	0.4	10.1	80.8	0.5	67.8	107.0	0.5	8.5	48.7	0.5	10.8
50	67.7	0.5	50.3	80.9	0.5	336.3	106.8	0.5	42.7	48.8	0.6	54.6
100	67.4	0.3	101.0	81.5	0.5	678.7	106.8	0.5	85.7	48.8	0.7	109.3

Compound **MS 21–11** exhibits the highest binding affinity according to MM-PBSA calculations (Table 4). This is supported by the multiple strong interactions, it forms with the protein. **MS 21–11** forms π–π stacking interactions between the cyclohexane and cyclopentane rings with Phe292, and Tyr334. Additionally, it has hydrogen bonds with Gly117, Gly118, Tyr130, and Glu199 interacting with the hydroxy group at position 4 of the benzene ring, **MS 21–11** also shows hydrophobic interactions with Trp83 and Phe335, as demonstrated in Fig. 4.

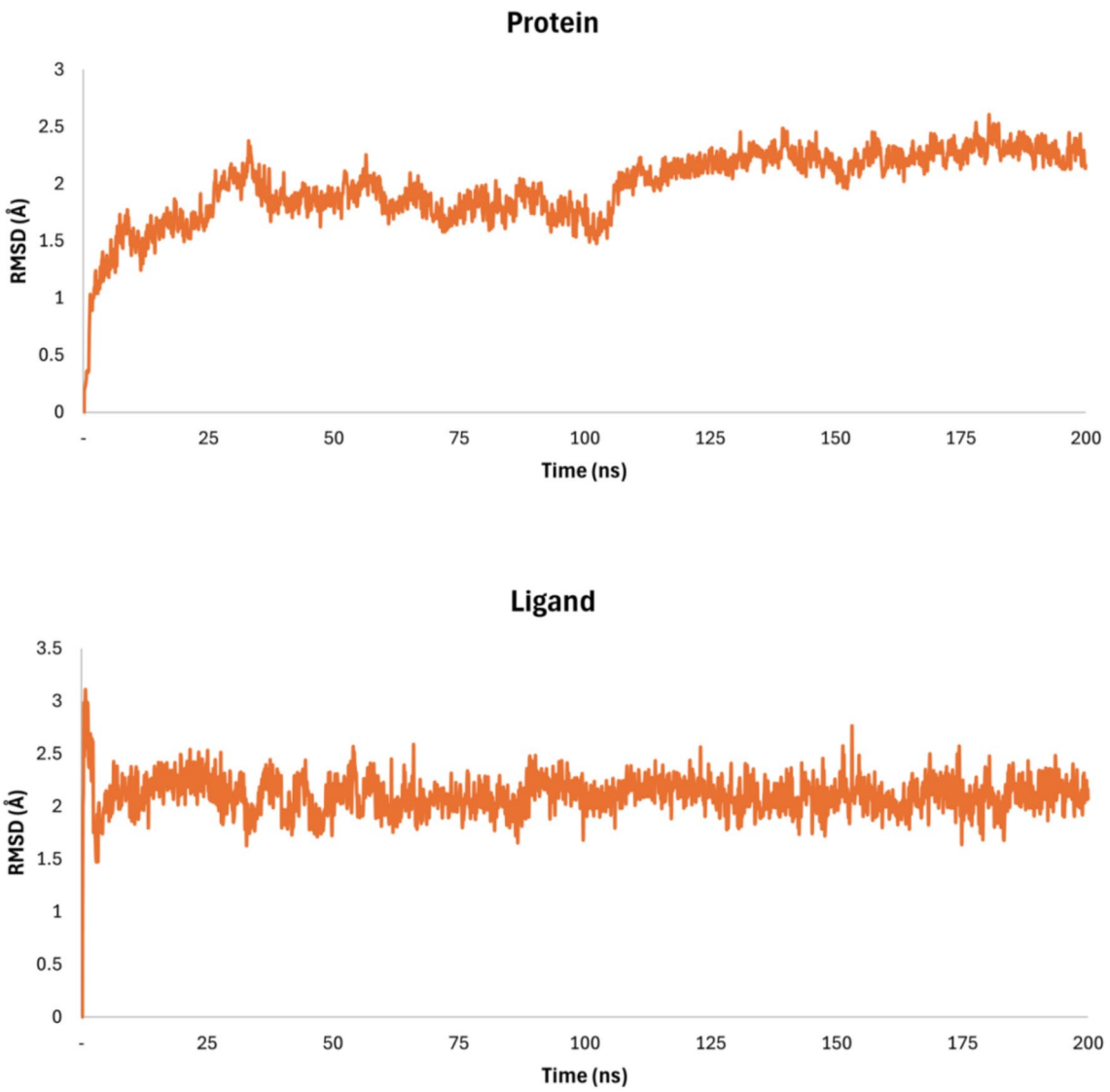

Fig. 3 Protein and ligand RMSD (Å) indicating stable confirmation throughout the simulation run of 200 ns

Table 4 Average SASA (Å2), Percentage of SASA for the buried ligand, total binding energy and average Per-residue decomposition of the MM-PBSA values obtained for the selected ligands in complex with human acetylcholinesterase

Ligand	Average SASA (Å^2)	% of Ligand buried	ΔGbind (kcal/mol)	Main contributors (kcal/mol)
Reference ligand (E20)	685.9 ± 11.6	77.9	− 28.9 ± 0.1	LEU73 (− 1.3 ± 0.9), TPR83 (− 0.2 ± 0.3), GLY118 (− 0.7 ± 0.4), TRP283 (− 2.1 ± 1.1), VAL291 (− 0.7 ± 0.5) PHE292 (− 0.2 ± 0.2, PHE294 (− 0.8 ± 0.3), PHE335 (− 1.1 ± 0.6), TYR338 (− 1.8 ± 0.7)
MS 21–11	487.1 ± 9.6	92.8	− 36.6 ± 0.1	TRP83 (− 2.9 ± 0.5), GLY117 (− 1.2 ± 0.3), GLY118 (− 1.2 ± 0.5), GLU199 (− 3.1 ± 0.7), SER200 (− 1.9 ± 0.4), TYR334 (− 1.9 ± 0.5), PHE335 (− 1.0 ± 0.4), HIS444 (− 1.8 ± 0.5)

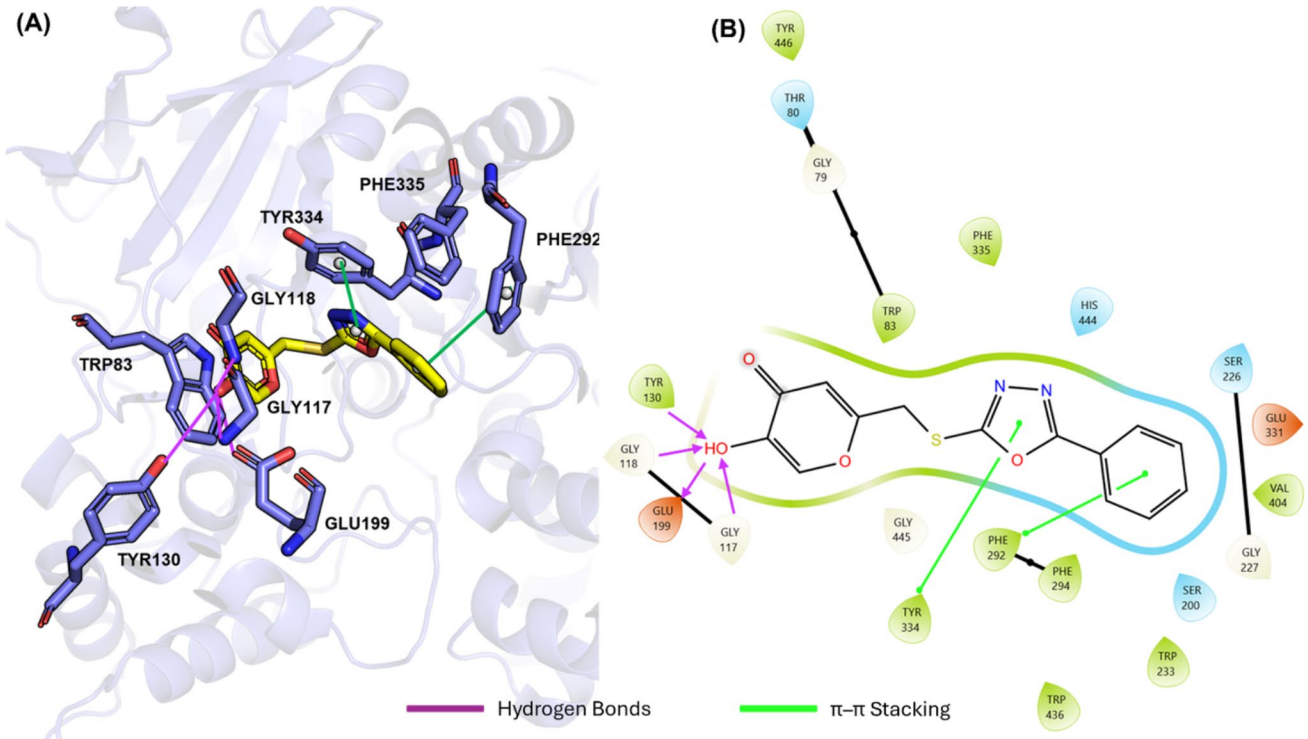

Fig. 4 Predicted molecular interaction diagrams for MS 21–11 in complex with human acetylcholinesterase (hAChE): 3D interaction diagram, ligand (yellow colour), amino acid residues (blue colour) (**A**) and 2D interaction diagram (**B**). These figures were generated using PyMOL (Delano 2002) and Maestro (Sankar et al. 2022)

Conclusion

In conclusion, the present research demonstrates the potential of kojic acid-based heteroaryl thiol-linked derivatives as novel acetylcholinesterase inhibitors for Alzheimer's disease therapy. Synthesized compounds exhibited promising in vitro AChE inhibition and anti-amyloid-β aggregation properties, with **MS 21–05** and **MS 21–11** emerging as the most potent candidates. Both compounds also demonstrated favorable BBB permeability. Moreover, molecular docking and molecular dynamics simulations of compound **MS 21–11** at the AChE-PAS site exhibited interactions with the amino acid residues essential for its inhibitory activity, maintaining stable conformation during the 200 ns simulation period. Overall, these key findings underscore therapeutic potency of kojic acid derivatives as dual-action components, addressing both cholinergic dysfunction and amyloid plaque formation in AD, and paving the way for further optimization of these promising lead molecules.

Supplementary Information The online version contains supplementary material available at https://doi.org/10.1007/s13205-025-04295-5.

Acknowledgements The authors express their gratitude to Indira Gandhi National Tribal University, Amarkantak, for the facilities made available for this research and Mr. Madan Singh wishes to acknowledge IGNTU, Amarkantak for providing fellowship.

Data availability The data that support the findings of this study are available from the corresponding author, [NSHNM], upon reasonable request.

Declarations

Conflict of interest The authors declare no conflicts of interest.

References

Abdallah AE (2024) Review on anti-alzheimer drug development: approaches, challenges and perspectives. RSC Adv 14(16):11057–11088. https://doi.org/10.1039/D3RA08333K

Ana Paula M, Maria Belen F, María Julia C, Natalia Paola A, Valeria C (2013) Natural AChE inhibitors from plants and their contribution to Alzheimer's disease therapy. Curr Neuropharmacol 11(4):388–413. https://doi.org/10.2174/1570159X11311040004

Babaee S, Chehardoli G, Akbarzadeh T, Zolfigol MA, Mahdavi M, Rastegari A, HomayouniMoghadam F, Najafi Z (2021) Design, synthesis, and molecular docking of some novel tacrine based cyclopentapyranopyridine- and tetrahydropyranoquinoline-kojic acid derivatives as anti-acetylcholinesterase agents. Chem Biodivers 18(6):e2000924. https://doi.org/10.1002/cbdv.202000924

Bell EW, Zhang Y (2019) DockRMSD: an open-source tool for atom mapping and RMSD calculation of symmetric molecules through graph isomorphism. J Cheminform 11(1):40. https://doi.org/10.1186/s13321-019-0362-7

Brtko J (2022) Biological functions of kojic acid and its derivatives in medicine, cosmetics, and food industry: Insights into health aspects. Arch Pharm 355(10):2200215. https://doi.org/10.1002/ardp.202200215

Case DA, Cheatham TE 3rd, Darden T, Gohlke H, Luo R, Merz KM Jr, Onufriev A, Simmerling C, Wang B, Woods RJ (2005) The Amber biomolecular simulation programs. J Comput Chem 26(16):1668–1688. https://doi.org/10.1002/jcc.20290

Darsey JA, Masarweh N (2020) Computational modelling of drugs for Alzheimer's disease (AD) and applications on artificial neural network systems (ANN); NETS. Pharmacy & Pharmacology International Journal Delano WL The PyMOL Molecular Graphics System. In, 2002

DeTure MA, Dickson DW (2019) The neuropathological diagnosis of Alzheimer's disease. Mol Neurodegener 14(1):32. https://doi.org/10.1186/s13024-019-0333-5

Di L, Kerns EH, Fan K, McConnell OJ, Carter GT (2003) High throughput artificial membrane permeability assay for blood–brain barrier. Eur J Med Chem 38(3):223–232. https://doi.org/10.1016/S0223-5234(03)00012-6

Ellman GL, Courtney KD, Andres V, Featherstone RM (1961) A new and rapid colorimetric determination of acetylcholinesterase activity. Biochem Pharmacol 7(2):88–95. https://doi.org/10.1016/0006-2952(61)90145-9

Emami S, Ahmadi R, Ahadi H, Ashooriha M (2022) Diverse therapeutic potential of 3-hydroxy-4-pyranones and related compounds as kojic acid analogs. Med Chem Res 31(11):1842–1861. https://doi.org/10.1007/s00044-022-02954-3

Fan L, Mao C, Hu X, Zhang S, Yang Z, Hu Z, Sun H, Fan Y, Dong Y, Yang J, Shi C, Xu Y (2020) New insights into the pathogenesis of Alzheimer's disease. Front Neurol. https://doi.org/10.3389/fneur.2019.01312

Foret MK, Orciani C, Welikovitch LA, Huang C, Cuello AC, Do Carmo S (2024) Early oxidative stress and DNA damage in Aβ-burdened hippocampal neurons in an Alzheimer's-like transgenic rat model. Communications Biology 7(1):861. https://doi.org/10.1038/s42003-024-06552-4

García-Ayllón M-S, Small DH, Avila J, Saez-Valero J (2011) Revisiting the role of acetylcholinesterase in Alzheimer's disease: cross-talk with P-tau and β-Amyloid. Front Mol Neurosci. https://doi.org/10.3389/fnmol.2011.00022

Gerlits O, Ho KY, Cheng X, Blumenthal D, Taylor P, Kovalevsky A, Radić Z (2019) A new crystal form of human acetylcholinesterase for exploratory room-temperature crystallography studies. Chem Biol Interact 309:108698. https://doi.org/10.1016/j.cbi.2019.06.011

He M, Fan M, Liu W, Li Y, Wang G (2021) Design, synthesis, molecular modeling, and biological evaluation of novel kojic acid derivatives containing bioactive heterocycle moiety as inhibitors of tyrosinase and antibrowning agents. Food Chem 362:130241. https://doi.org/10.1016/j.foodchem.2021.130241

Miller BR III, McGee TD Jr, Swails JM, Homeyer N, Gohlke H, Roitberg AE (2012) MMPBSA.py: an efficient program for end-state free energy calculations. J Chem Theory Comp 8(9):3314–3321. https://doi.org/10.1021/ct300418h

Nichols E, Steinmetz JD, Vollset SE, Fukutaki K, Chalek J, Abd-Allah F, Abdoli A, Abualhasan A, Abu-Gharbieh E, Akram TT, Al Hamad H, Alahdab F, Alanezi FM, Alipour V, Almustanyir S, Amu H, Ansari I, Arabloo J, Ashraf T, Astell-Burt T, Ayano G, Ayuso-Mateos JL, Baig AA, Barnett A, Barrow A, Baune BT, Béjot Y, Bezabhe WMM, Bezabih YM, Bhagavathula AS, Bhaskar S, Bhattacharyya K, Bijani A, Biswas A, Bolla SR, Boloor A, Brayne C, Brenner H, Burkart K, Burns RA, Cámera LA, Cao C, Carvalho F, Castro-de-Araujo LFS, Catalá-López F, Cerin E, Chavan PP, Cherbuin N, Chu D-T, Costa VM, Couto RAS, Dadras O, Dai X, Dandona L, Dandona R, De la Cruz-Góngora V, Dhamnetiya D, Dias da Silva D, Diaz D, Douiri A, Edvardsson D, Ekholuenetale M, El Sayed I, El-Jaafary SI, Eskandari K, Eskandarieh S, Esmaeilnejad S, Fares J, Faro A, Farooque U, Feigin VL, Feng X, Fereshtehnejad S-M, Fernandes E, Ferrara P, Filip I, Fillit H, Fischer F, Gaidhane S, Galluzzo L, Ghashghaee A, Ghith N, Gialluisi A, Gilani SA, Glavan I-R, Gnedovskaya EV, Golechha M, Gupta R, Gupta VB, Gupta VK, Haider MR, Hall BJ, Hamidi S, Hanif A, Hankey GJ, Haque S, Hartono RK, Hasaballah AI, Hasan MT, Hassan A, Hay SI, Hayat K, Hegazy MI, Heidari G, Heidari-Soureshjani R, Herteliu C, Househ M, Hussain R, Hwang B-F, Iacoviello L, Iavicoli I, Ilesanmi OS, Ilic IM, Ilic MD, Irvani SSN, Iso H, Iwagami M, Jabbarinejad R, Jacob L, Jain V, Jayapal SK, Jayawardena R, Jha RP, Jonas JB, Joseph N, Kalani R, Kandel A, Kandel H, Karch A, Kasa AS, Kassie GM, Keshavarz P, Khan MAB, Khatib MN, Khoja TAM, Khubchandani J, Kim MS, Kim YJ, Kisa A, Kisa S, Kivimäki M, Koroshetz WJ, Koyanagi A, Kumar GA, Kumar M, Lak HM, Leonardi M, Li B, Lim SS, Liu X, Liu Y, Logroscino G, Lorkowski S, Lucchetti G, LutzkySaute R, Magnani FG, Malik AA, Massano J, Mehndiratta MM, Menezes RG, Meretoja A, Mohajer B, Mohamed Ibrahim N, Mohammad Y, Mohammed A, Mokdad AH, Mondello S, Moni MAA, Moniruzzaman M, Mossie TB, Nagel G, Naveed M, Nayak VC, NeupaneKandel S, Nguyen TH, Oancea B, Otstavnov N, Otstavnov SS, Owolabi MO, Panda-Jonas S, PashazadehKan F, Pasovic M, Patel UK, Pathak M, Peres MFP, Perianayagam A, Peterson CB, Phillips MR, Pinheiro M, Piradov MA, Pond CD, Potashman MH, Pottoo FH, Prada SI, Radfar A, Raggi A, Rahim F, Rahman M, Ram P, Ranasinghe P, Rawaf DL, Rawaf S, Rezaei N, Rezapour A, Robinson SR, Romoli M, Roshandel G, Sahathevan R, Sahebkar A, Sahraian MA, Sathian B, Sattin D, Sawhney M, Saylan M, Schiavolin S, Seylani A, Sha F, Shaikh MA, Shaji KS, Shannawaz M, Shetty JK, Shigematsu M, Shin JI, Shiri R, Silva DAS, Silva JP, Silva R, Singh JA, Skryabin VY, Skryabina AA, Smith AE, Soshnikov S, Spurlock EE, Stein DJ, Sun J, Tabarés-Seisdedos R, Thakur B, Timalsina B, Tovani-Palone MR, Tran BX, Tsegaye GW, Valadan-Tahbaz S, Valdez PR, Venketasubramanian N, Vlassov V, Vu GT, Vu LG, Wang Y-P, Wimo A, Winkler AS, Yadav L, Yahyazadeh Jabbari SH, Yamagishi K, Yang L, Yano Y, Yonemoto N, Yu C, Yunusa I, Zadey S, Zastrozhin MS, Zastrozhina A, Zhang Z-J, Murray CJL, Vos T (2022) Estimation of the global prevalence of dementia in 2019 and forecasted prevalence in 2050: an analysis for the Global Burden of Disease Study 2019. Lancet Public Health 7(2):e105–e125. https://doi.org/10.1016/S2468-2667(21)00249-8

Obaid RJ, Naeem N, Mughal EU, Al-Rooqi MM, Sadiq A, Jassas RS, Moussa Z, Ahmed SA (2022) Inhibitory potential of nitrogen, oxygen and sulfur containing heterocyclic scaffolds against acetylcholinesterase and butyrylcholinesterase. RSC Adv 12(31):19764–19855. https://doi.org/10.1039/D2RA03081K

O'Boyle NM, Banck M, James CA, Morley C, Vandermeersch T, Hutchison GR (2011) Open babel: an open chemical toolbox. J Cheminform 3(1):33. https://doi.org/10.1186/1758-2946-3-33

Peauger L, Azzouz R, Gembus V, Ţînţaş M-L, Sopková-de Oliveira Santos J, Bohn P, Papamicaël C, Levacher V (2017) Donepezil-based central acetylcholinesterase inhibitors by means of a "bio-oxidizable" prodrug strategy: design, synthesis, and in vitro biological evaluation. J Med Chem 60(13):5909–5926. https://doi.org/10.1021/acs.jmedchem.7b00702

Rai SN, Singh C, Singh A, Singh MP, Singh BK (2020) Mitochondrial dysfunction: a potential therapeutic target to treat Alzheimer's

disease. Mol Neurobiol 57(7):3075–3088. https://doi.org/10.1007/s12035-020-01945-y

Rakse M, Karthikeyan C, Deora GS, Moorthy NSHN, Rathore V, Rawat AK, Srivastava AK, Trivedi P (2013) Design, synthesis and molecular modelling studies of novel 3-acetamido-4-methyl benzoic acid derivatives as inhibitors of protein tyrosine phosphatase 1B. Eur J Med Chem 70:469–476. https://doi.org/10.1016/j.ejmech.2013.10.030

Ramakrishna K, Karuturi P, Siakabinga Q, T.A. G, Krishnamurthy S, Singh S, Kumari S, Kumar GS, Sobhia ME, Rai SN (2024) Indole-3 Carbinol and Diindolylmethane Mitigated β-Amyloid-Induced Neurotoxicity and Acetylcholinesterase Enzyme Activity: In Silico, In Vitro, and Network Pharmacology Study. Diseases 12 (8):184

Ramrao SP, Verma A, Waiker DK, Tripathi PN, Shrivastava SK (2021) Design, synthesis, and evaluation of some novel biphenyl imidazole derivatives for the treatment of Alzheimer's disease. J Mol Struct 1246:131152. https://doi.org/10.1016/j.molstruc.2021.131152

Saeedi M, Eslamifar M, Khezri K (2019) Kojic acid applications in cosmetic and pharmaceutical preparations. Biomed Pharmacother 110:582–593. https://doi.org/10.1016/j.biopha.2018.12.006

Sankar K, Trainor K, Blazer LL, Adams JJ, Sidhu SS, Day T, Meiering E, Maier JKX (2022) A descriptor set for quantitative structure-property relationship prediction in biologics. Mol Inf 41(9):2100240. https://doi.org/10.1002/minf.202100240

Shrivastava SK, Nivrutti AA, Bhardwaj B, Waiker DK, Verma A, Tripathi PN, Tripathi M, Saraf P (2022) Drug reposition-based design, synthesis, and biological evaluation of dual inhibitors of acetylcholinesterase and β-Secretase for treatment of Alzheimer's disease. J Mol Struct 1262:132979. https://doi.org/10.1016/j.molstruc.2022.132979

Silva D, Chioua M, Samadi A, Agostinho P, Garção P, Lajarín-Cuesta R, De Los RC, Iriepa I, Moraleda I, Gonzalez-Lafuente L, Mendes E, Pérez C, Rodríguez-Franco MI, Marco-Contelles J, CarmoCarreiras M (2013) Synthesis, pharmacological assessment, and molecular modeling of acetylcholinesterase/butyrylcholinesterase inhibitors: effect against amyloid-β-induced neurotoxicity. ACS Chem Neurosci 4(4):547–565. https://doi.org/10.1021/cn300178k

Singh YP, Shankar G, Jahan S, Singh G, Kumar N, Barik A, Upadhyay P, Singh L, Kamble K, Singh GK, Tiwari S, Garg P, Gupta S, Modi G (2021) Further SAR studies on natural template based neuroprotective molecules for the treatment of Alzheimer's disease. Bioorg Med Chem 46:116385. https://doi.org/10.1016/j.bmc.2021.116385

Srivastava P, Tripathi PN, Sharma P, Rai SN, Singh SP, Srivastava RK, Shankar S, Shrivastava SK (2019) Design and development of some phenyl benzoxazole derivatives as a potent acetylcholinesterase inhibitor with antioxidant property to enhance learning and memory. Eur J Med Chem 163:116–135. https://doi.org/10.1016/j.ejmech.2018.11.049

Taylor P, Lwebuga-Mukasa J, Lappi S, Rademacher J (1974) Propidium—a fluorescence probe for a peripheral anionic site on acetylcholinesterase. Mol Pharmacol 10(4):703–708

Tripathi PN, Srivastava P, Sharma P, Tripathi MK, Seth A, Tripathi A, Rai SN, Singh SP, Shrivastava SK (2019) Biphenyl-3-oxo-1,2,4-triazine linked piperazine derivatives as potential cholinesterase inhibitors with anti-oxidant property to improve the learning and memory. Bioorg Chem 85:82–96. https://doi.org/10.1016/j.bioorg.2018.12.017

Tripathi PN, Lodhi A, Rai SN, Nandi NK, Dumoga S, Yadav P, Tiwari AK, Singh SK, El-Shorbagi AA, Chaudhary S (2024) Review of pharmacotherapeutic targets in Alzheimer's disease and its management using traditional medicinal plants. Degener Neurol Neuromuscul Dis 14:47–74. https://doi.org/10.2147/dnnd.S452009

Tsinman O, Tsinman K, Sun N, Avdeef A (2011) Physicochemical selectivity of the BBB microenvironment governing passive diffusion—matching with a porcine brain lipid extract artificial membrane permeability model. Pharm Res 28(2):337–363. https://doi.org/10.1007/s11095-010-0280-x

Verdonk ML, Cole JC, Hartshorn MJ, Murray CW, Taylor RD (2003) Improved protein-ligand docking using GOLD. Proteins 52(4):609–623. https://doi.org/10.1002/prot.10465

Verma A, Waiker DK, Singh N, Singh A, Saraf P, Bhardwaj B, Kumar P, Krishnamurthy S, Srikrishna S, Shrivastava SK (2024) Lead optimization based design, synthesis, and pharmacological evaluation of quinazoline derivatives as multi-targeting agents for Alzheimer's disease treatment. Eur J Med Chem 271:116450. https://doi.org/10.1016/j.ejmech.2024.116450

Vu M, Mangal R, Stead T, Lopez-Ortiz C, Ganti L (2022) Impact of Alzheimer's disease on caregivers in the united states. Health Psychol Res 10(3):37454. https://doi.org/10.52965/001c.37454

Waiker DK, Verma A, Akhilesh AGT, Singh N, Roy A, Dilnashin H, Tiwari V, Trigun SK, Singh SP, Krishnamurthy S, Lama P, Davisson VJ, Shrivastava SK (2023) Design, synthesis, and biological evaluation of piperazine and N-Benzylpiperidine hybrids of 5-phenyl-1,3,4-oxadiazol-2-thiol as potential multitargeted ligands for Alzheimer's disease therapy. ACS Chem Neurosci 14(11):2217–2242. https://doi.org/10.1021/acschemneuro.3c00245

Waiker DK, Verma A, Gajendra TA, Namrata RA, Kumar P, Trigun SK, Srikrishna S, Krishnamurthy S, Davisson VJ, Shrivastava SK (2024) Design, synthesis, and biological evaluation of some 2-(3-oxo-5,6-diphenyl-1,2,4-triazin-2(3H)-yl)-N-phenylacetamide hybrids as MTDLs for Alzheimer's disease therapy. Eur J Med Chem 271:116409. https://doi.org/10.1016/j.ejmech.2024.116409

Wang J, Wolf RM, Caldwell JW, Kollman PA, Case DA (2004) Development and testing of a general amber force field. J Comput Chem 25(9):1157–1174. https://doi.org/10.1002/jcc.20035

Zuin M, Cherubini A, Volpato S, Ferrucci L, Zuliani G (2022) Acetylcholinesterase-inhibitors slow cognitive decline and decrease overall mortality in older patients with dementia. Sci Rep 12(1):12214. https://doi.org/10.1038/s41598-022-16476-w